



Contents lists available at ScienceDirect

Arabian Journal of Chemistry

journal homepage: www.ksu.edu.sa

Plasma protein affinity, antioxidant, and anti-lung cancer properties of O-methylated flavonol rhamnazin

Zheng Chen^{a,1}, Yan Qiao^{a,1}, Yu Chen^b, Tingting Ma^a, Wei Li^a, Jianhong Xia^a, Yan Yan^a, Qian Jiang^a, Liqing Zhou^{a,*}

^a Department of Radiation Oncology, Huai'an Hospital Affiliated to Xuzhou Medical University, Huaian, 223001, China

^b Department of Oncology, Huai'an Hospital Affiliated to Xuzhou Medical University, Huaian, 223001, China

ARTICLE INFO

Keywords:

Rhamnazin
Human serum albumin
Interaction
Antioxidant
Anticancer

ABSTRACT

Medicinal herbs can be used for the development of antioxidant and anticancer platforms. However, the mechanisms by which the bioactive materials show these properties remain largely unclear. Also, a detailed understanding of the interaction between small compounds and carrier proteins like albumin can provide useful information about the regulation of their stability and circulation time properties. In this paper, the interaction of rhamnazin (C₁₇H₁₄O₇), an O-methylated flavonol exists in *Rhamnus petiolaris*, with human serum albumin (HSA) was investigated. Also, the antioxidant and anti-lung cancer effects of rhamnazin were assessed. The results showed that a static rhamnazin-HSA complex was formed by the contribution of hydrophobic forces, which led to an increase in the content of the α -helix structure of HSA. Cellular assays revealed that rhamnazin (10 μ M) recovered cell viability in human proximal renal tubular epithelial cells (HK2) reduced by H₂O₂ (0.5 mM) through reduction of ROS, restoration of CAT and SOD activities and GSH content, regulation of Bax, Bcl-2, and caspase-3. Moreover, the anti-lung cancer data demonstrated that rhamnazin induced apoptosis on lung adenocarcinoma A549 cells associated with a p53-dependent manner via overexpression of apoptotic Bax and caspase-3 and down-regulation of anti-apoptotic Bcl-2. To summarize, the potential binding of rhamnazin and HSA, as well as its antioxidant/anticancer properties, are critical for understanding the solubility and stability of this bioactive compound in plasma, as well as its therapeutic implications.

1. Introduction

Oxidative stress has been widely shown to be involved in the onset of several diseases including chronic diseases (Jomova, Raptova et al. 2023) and cancer (Iqbal, Kabeer et al. 2024). Oxidative stress driving from the dysregulation of endogenous oxidant signaling pathways results in overproduction of reactive oxygen species (ROS) (Aguilar, Navarro et al. 2016). For example, it has been shown that kidney proximal tubular epithelial cells are highly sensitive to ROS-triggered adverse effects (Kishi, Nagasu et al. 2024). Chronic kidney disorder has been documented as a spreading disease worldwide, with ongoing conventional therapeutics platforms showing limited potential efficacy (Yuan, Tang et al. 2022). Some alternative approaches to promisingly inhibit the progression of kidney disorder may provide useful outcomes for patients suffering from this disease.

On the other hand, because of the wide range of signs and symptoms,

non-small cell lung cancer (NSCLC) represents a heterogeneous disease that is typically detected at an advanced stage. Over the past decade, we have seen an increase in the overall number of patients suffering from NSCLC, which has driven researchers to devote themselves to the development of potential anticancer systems. In fact, NSCLC is known as the leading cause of cancer-related fatalities globally, and the frequency of newly diagnosed cases has increased in China in recent years (Chen, Liu et al. 2022).

Rhamnazin (C₁₇H₁₄O₇) is known as an O-methylated flavonoid present in *Rhamnus petiolaris*, and has shown potential antioxidant activity (Patel, Kumar et al. 2018). For example, Wu et al. showed that rhamnazin provides antioxidant and anti-inflammatory impacts against lipopolysaccharide-triggered acute lung injury *in vivo* (Wu, Dai et al. 2017). Furthermore, Yang et al. demonstrated that rhamnazin reduces traumatic brain injury *in vivo* through the regulation of oxidative stress (Yang, Zhang et al. 2022). Moreover, rhamnazin mitigates

* Corresponding author at: Huaian Hospital Affiliated to Xuzhou Medical University, 62 South Huaihai Road, Huaian 223001, China.

E-mail address: zfq-hill@163.com (L. Zhou).

¹ The authors equally contributed to this work.

<https://doi.org/10.1016/j.arabjc.2024.105891>

Received 5 June 2024; Accepted 28 June 2024

Available online 2 July 2024

1878-5352/© 2024 The Author(s). Published by Elsevier B.V. on behalf of King Saud University. This is an open access article under the CC BY-NC-ND license (<http://creativecommons.org/licenses/by-nc-nd/4.0/>).

lipopolysaccharide-stimulated inflammation and oxidative stress in raw macrophages (Kim 2016).

Regarding the anticancer properties of rhamnazin, Yu et al. reported that this small molecule can serve as a potential modulator of the VEGFR2 signaling pathway with promising antiangiogenic and anti-tumor efficiencies (Yu, Cai et al. 2015). Also, Mei et al. showed that rhamnazin inhibits hepatocellular carcinoma cell proliferation through glutathione peroxidase 4-dependent ferroptosis (Mei, Liu et al. 2022).

Small molecules are mostly transported in the body by human serum albumin (HSA) protein. HSA as a multifunctional protein has been reported to act as a versatile small molecule carrier for the regulation of several disorders (Chen and Liu 2016, Ghosh and Bhadra 2024). HSA with a flexible structure carries a number of compounds, such as bilirubin, fatty acids, amino acids, hormones, drugs, antibiotics, small compounds, and several metal cations (Quinlan, Martin et al. 2005, Kratz 2014). The interaction of small molecules with HSA not only regulates their pharmacokinetic properties but also the probable protein structural change can be one of the causes of their side effects (Yamasaki, Chuang et al. 2013, Tayyab and Feroz 2021). Therefore, the interaction of different small molecules with HSA has been widely reported in different studies (Siddiqui, Ameen et al. 2021). The secondary structure of HSA does not usually change, but its tertiary conformation, which includes the special arrangement of atoms in three-dimensional space, may undergo some significant changes upon interaction with ligands (Siddiqui, Ameen et al. 2021). In other words, HSA has a unique spatial conformation as a result of protein folding, which can play a key role in the physiological function of this protein (Ghosh and Bhadra 2024). Therefore, determining the thermodynamic and structural parameters of HSA upon interaction with small particles can provide useful information about the formation of ligand-HSA complexes and the underlying physiological properties of small molecules, which can be studied by different spectroscopic techniques (Zeinabad, Kachooei et al. 2016).

Therefore, the interaction of rhamnazin and HSA was studied by several spectroscopic techniques along with molecular docking study. Also, the protective effect of rhamnazin against cytotoxicity induced by H₂O₂ in HK2 cells was assessed by different cellular and molecular assays. Moreover, the anti-lung cancer properties of rhamnazin and the associated signaling pathway were assessed *in vitro*.

2. Materials and methods

2.1. Materials

Rhamnazin; 99 % (HPLC), HSA, Dulbecco's modified Eagle's medium (DMEM)/Ham's F12, fetal bovine serum (FBS), and tetrazolium dye 3-(4,5-dimethylthiazol-2-yl)-2,5-diphenyltetrazolium bromide (MTT) were purchased from Sigma (Saint Louis, MO, USA). Primary antibodies were purchased from Santa Cruz Biotechnology (Santa Cruz, CA). FITC Annexin V Apoptosis Detection Kit I was obtained from BD Biosciences (USA).

2.2. Sample preparation

The stock solution (100 μM) of HSA was freshly prepared in phosphate buffer (100 mM, pH 7.4). UV-visible spectroscopy was used to determine the protein concentration using $\epsilon_{1\text{cm}}^{\%}$ of 5.30 at 280 nm (Alam, Chaturvedi et al. 2015). Rhamnazin solution (4 mM) was prepared freshly in phosphate buffer (100 mM, pH 7.4) or cell culture medium with the addition of 1 % DMSO.

2.3. Intrinsic fluorescence quenching study

The intrinsic fluorescence quenching study was done using a fluorescence spectrophotometer (RF-5301 Shimadzu, Japan). The analysis was done at three different temperatures of 298/310/315 K with a

quartz cell of 0.1 cm path length. Excitation and emission slits were set at 5 and 10 nm, respectively, where the samples were excited at 280 nm and emission signals were read in the range of 300–420 nm. The titration of rhamnazin (5–40 μM) to HSA (5 μM) solution was performed at three different temperatures. The maximum fluorescence intensity was used to calculate the quenching, binding and thermodynamic parameters. All spectra were corrected against off-signals and inner filter effect (Ali and Al-Lohedan 2018).

2.4. Circular dichroism study

The far-UV CD study (200–260 nm) was performed using a JASCO-J 813 spectropolarimeter at room temperature. The quartz cell with a path length of 0.1 cm was used to detect the ellipticity changes in the HSA solution (5 μM) upon interaction with increasing concentrations of rhamnazin (5, 10, 15, 20, 30, 40). The CD data read from 200 to 260 nm were analyzed using CDNN.

2.5. Molecular docking study

Vina Autodock was used to perform the docking study. The 3D structures of HSA (PDB ID: 1AO6) and rhamnazin (PubChem CID: 5320945) were obtained from Protein Data Bank and PubChem, respectively. Water molecules as well as ions were removed, and hydrogen atoms and partial Kollman charges were added/assigned to rigid HSA. The grid size was set at 51 Å, 108 Å, 90 Å along X, Y, and Z axes, respectively. Spacing, mode number, energy range and exhaustiveness were fixed at 1, 10, 5 and 8, respectively.

2.6. Cell culture

Human proximal renal tubular epithelial cells (HK2, purchased from Procell Life Science and Technology Co., Wuhan, China) and lung adenocarcinoma A549 cells (purchased from ATCC) were cultured in DMEM/Ham's F12 and DMEM, respectively, supplemented with 10 % FBS, penicillin (1000 U/ml) and streptomycin (1000 U/ml) in 5 % CO₂ at 37 °C.

2.7. Treatments

A fixed concentration of H₂O₂ (0.5 mM) for 24 h was used to trigger apoptosis in HK2 cells based on the previous studies (Small, Morais et al. 2014, Shahzad, Small et al. 2016). Also, concentration-response assays (range 1–50 μM) were done to determine the maximum rhamnazin concentration that did not stimulate cytotoxicity in HK2 cells. Based on this pilot assay, a maximum safe concentration of 10 μM rhamnazin for HK2 cells at an incubation time of 24 h was determined. HK2 cells were then incubated for 24 h with H₂O₂ (0.5 mM) alone or co-incubated with H₂O₂ (0.5 mM) and rhamnazin (10 μM). For lung adenocarcinoma A549 cells, the cells were incubated with different concentrations of rhamnazin (1–50 μM) for 24 h.

2.8. MTT assay

MTT assay was done to assess the cell viability based on the previous study (Shahzad, Small et al. 2016). Briefly, the culture medium was replaced with 100 μL of fresh medium supplemented with MTT (0.5 mg/ml), incubated for 60 min, and followed by removal of the medium and replacement with 100 μL of DMSO. The absorbance was then determined at 570 nm using a microplate reader (RT-2100C Microplate Reader, China).

2.9. Determination of oxidative stress

To analyze the formation of intracellular ROS, the HK2 cells incubated with different samples were added by 2,7-

dichlorodihydrofluorescein diacetate acetyl ester (H₂DCFDA) (10 mM) for 60 min at 37 °C. Then, the cells were washed with PBS and the fluorescence intensity of samples was detected using a fluorescence microplate reader (Bio-Tek Instruments, Winooski, USA) by excitation and emission wavelengths of 485 and 528 nm, respectively. CAT activity (Abcam, ab83464), SOD activity (Abcam, ab65354), and GSH content (Abcam, ab239709) in HK2 cells were examined following the product manual.

2.10. Quantitative real-time PCR

The relative expression of Bax, Bcl-2, and caspase-3 mRNA in HK2 cells and relative expression of Bax, Bcl-2, caspase-3, and p53 mRNA in A549 cell was assessed by quantitative real-time PCR following standard methods (Kong, Zhang et al. 2017, Yuan, Yang et al. 2021). Briefly, RNA from cells were extracted using Trizol kit (Invitrogen, CA, USA) and was reverse-transcribed using a Revert Aid First Strand cDNA Synthesis kit (Bio-Rad, CA, USA) following the product manual. The relative expression of mRNA was assessed through real-time PCR using SYBR green master mix. The primer sequences were used as reported in the previous studies (Kong, Zhang et al. 2017, Yuan, Yang et al. 2021). The data was analyzed through the $2^{-\Delta\Delta Ct}$ method and GAPDH was used as the target gene to normalize data.

2.11. Western blot analysis

Western blot analysis was done based on the previous study (Shahzad, Small et al. 2016). Briefly, the HK2 cells were washed, scraped with RIPA cell lysis buffer supplemented with phosphatase and protease inhibitors, sonicated, and centrifuged (3,000g, 20 min, 4 °C). Protein concentration was calculated based on the Bradford assay. Then protein samples were run on an SDS-polyacrylamide gel (12 %), transferred onto PVDF membrane, soaked in a blocking buffer for 60 min for 1 h, and incubated with primary antibodies (1:1000) 24 h at 4 °C. Afterwards, the membrane was washed and added by anti-rabbit HRP-conjugated secondary antibody (1:2000). Finally, protein bands were detected using enhanced chemiluminescence.

2.12. Apoptosis induction

The apoptotic A549 cells after exposure to rhamnazin (IC₅₀ concentration) for 24 h was assessed using FITC Annexin V Apoptosis Detection Kit I according to the manufacturer's protocol and instructions reported previously (Akram, Al-Saffar et al. 2022). Briefly, after exposure, the A549 cells were collected, resuspended in the binding buffer, stained, and incubated in the dark place for 15 min. at room temperature. Cells were screened using flow cytometry (FACS ARIA III, BD Biosciences).

2.13. Determination of the level of expression of p53, Bcl-2, and Bax

Rhamnazin (IC₅₀ concentration)-treated and -untreated A549 cells were lysed. The level of expression of caspase-3, p53, Bax, and Bcl-2 was analyzed through colorimetric assays using human p53 ELISA kit (ab171571), human cleaved caspase-3 (Asp175) ELISA Kit (ab220655), human Bcl-2 ELISA kit (ab119506) and human Bax ELISA kit (ab199080), according to the protocols provided by the manufacturer. The expression of proteins was determined by detecting the absorbance at 450 nm using a microplate reader (RT-2100C Microplate Reader, China).

2.14. Statistical analysis

Data were presented as mean ± standard deviation of triplicate experiments for cellular assays (n = 3). Statistical analyses were analyzed with one-way ANOVA, followed by Tukey's test. Statistical significance

was set at P < 0.05.

3. Results and discussion

The investigation of interactions between rhamnazin with HSA has not been fully investigated in the literature. Therefore, we tried to analyze the interactions of rhamnazin with HSA using different spectroscopic techniques. The analysis was done to explore the quenching mechanism, thermodynamic and binding parameters, and structural changes of HSA. Collectively, we tried to analyze the biochemical interactions existing between HSA and rhamnazin and furnish a detailed characterization of the biological properties of rhamnazin.

3.1. Intrinsic fluorescence spectroscopy

Fluorescence spectroscopy is widely used to characterize ligand-macromolecule (protein/DNA) interaction mechanisms to provide details on the quenching mechanisms, binding parameters, as well as thermodynamic changes (Van de Weert and Stella 2011, dos Santos Rodrigues, Delgado et al. 2023). Principally, alterations in the intrinsic emission intensity of proteins are determined at the λ_{max} . The addition of rhamnazin to HSA results in the fluorescence quenching of HSA (excitation at 280 nm) at three different temperatures of 298/310/315 K with different quenching rates (Fig. 1).

The observed changes in fluorescence intensity patterns at different temperatures could be attributed to the reorganization of intra and intermolecular forces that contribute to protein stability and folding.

3.1.1. Quenching mechanism

Titration of rhamnazin to the HSA solution can lead to the potential interaction of this ligand with HSA and may form a complex (Kenoth and Kamlekar 2022). HSA fluorescence intensity was found to be quenched upon the addition of rhamnazin, concentration-dependently (Fig. 1). Quenching of HSA fluorescence emission with the addition of rhamnazin was assessed by the well-known Stern–Volmer Eq. (1) (Leilabadi-Asl, Divsalar et al. 2024):

$$F_0/F = 1 + K_{SV}[C] \quad (1)$$

where F_0 and F are defined as emission intensities of HSA before and after interaction with rhamnazin, respectively. K_{SV} and $[C]$ are the Stern–Volmer constant and the concentration of rhamnazin, respectively.

The Eq. (1) in Fig. 2a2a was plotted to determine the K_{SV} at three different temperatures of 298/310/315 K.

Fluorescence quenching can be categorized into three different classes: static, dynamic, or combined mechanisms, where they show different behaviors against temperature (Fossum, Johnson et al. 2023). The quenching constants under a dynamic quenching mechanism increase upon elevating temperatures, leading to large K_{SV} values. Nevertheless, higher temperatures can lead to a reduction in the stability of the formed complex, which can result in a decline in the K_{SV} values for static quenching. The formation of the static or dynamic complex is also can be verified using the calculation of quenching rate constant (k_q) values (Eq. (2)) (Roy, Tapan Kumar Das et al. 2016):

$$kq = K_{SV}/\tau_0 \quad (2)$$

where τ_0 is known as a constant revealing the average lifetime of the fluorophore in the excited state (10^{-8} s) (Roy, Tapan Kumar Das et al. 2016).

Fig. 2a displays the Stern–Volmer plot at three different temperatures of 298/310/315 K for the interaction of rhamnazin and HSA, and the resultant calculated K_{SV} and k_q values based on Eq. (1) and Eq. (2) are summarized in Table 1. Decreasing the K_{SV} values after increasing the system temperature revealed that the interaction of rhamnazin and HSA results in a static quenching mechanism. Furthermore, the order of

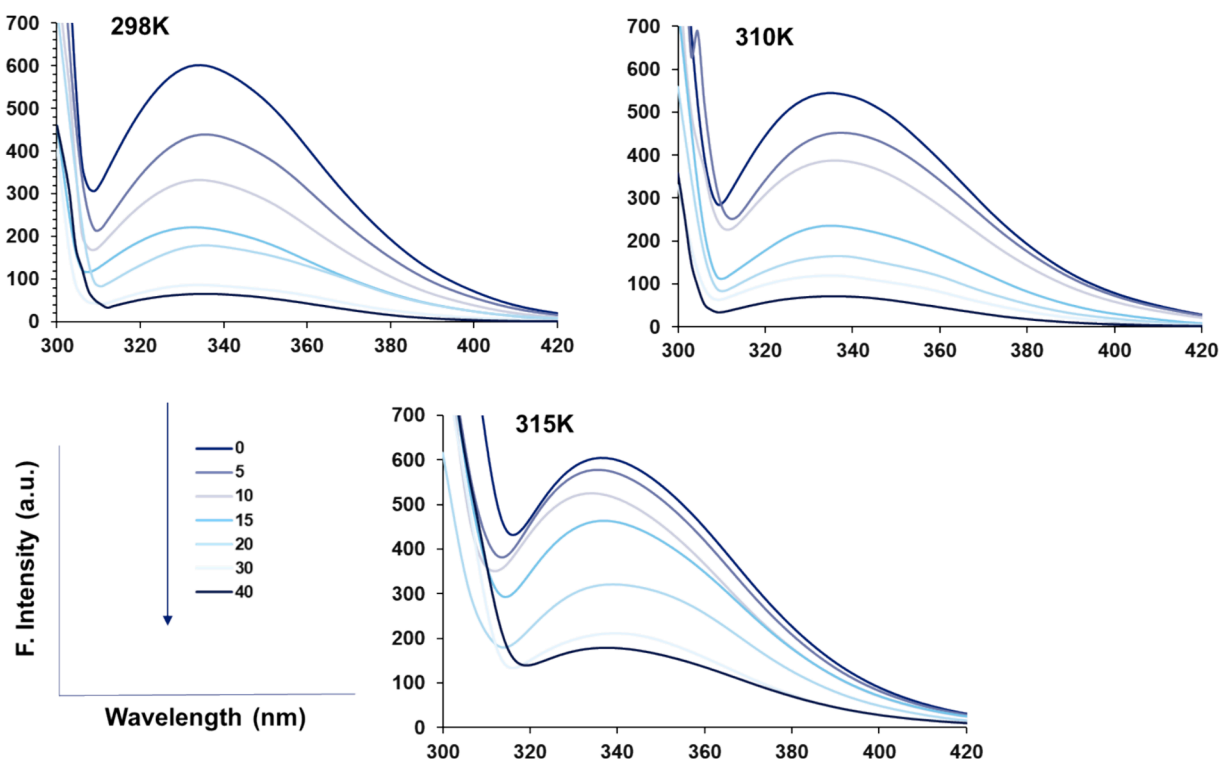


Fig. 1. Fluorescence quenching study of HSA (5 μM) upon interaction with different concentrations of rhamnazin ranging from 5 to 40 μM at three different temperatures of 298/310/315 K.

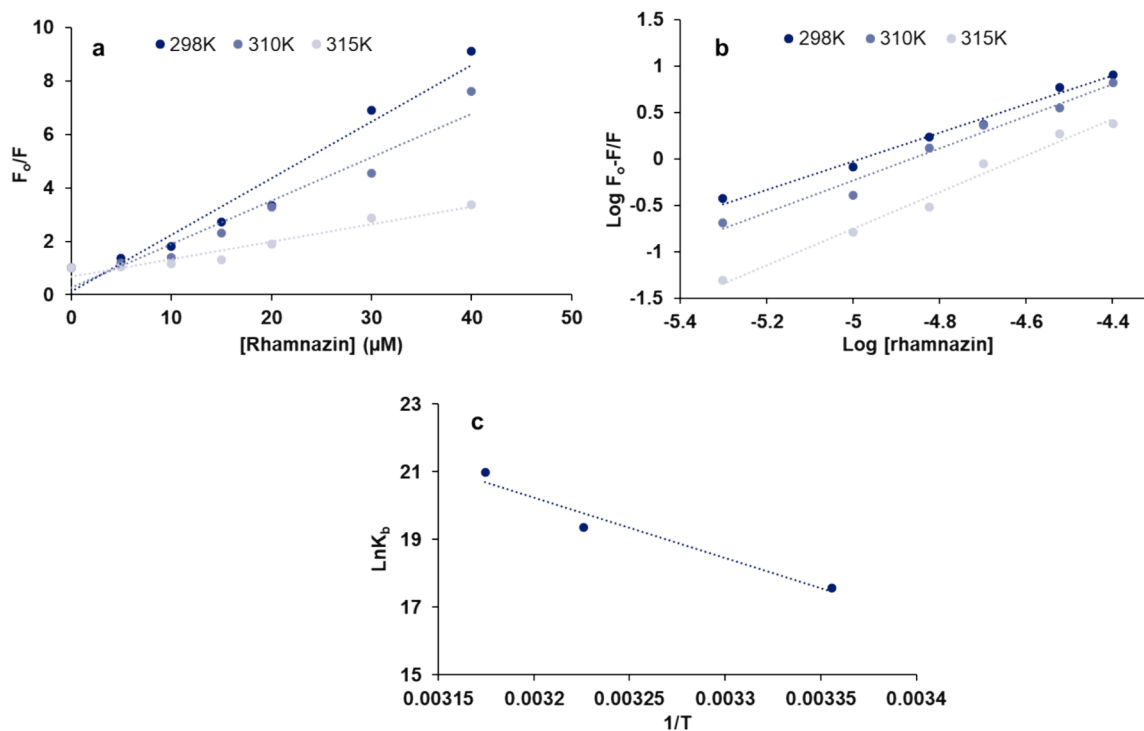


Fig. 2. (a) Stern-Volmer plot, (b) modified Stern-Volmer plot, (c) Van't Hoff plot for the interaction of HSA (5 μM) with different concentrations of rhamnazin ranging from 5 to 40 μM at three different temperatures of 298/310/315 K.

magnitude of the k_q for rhamnazin-complex was found to be 10^{13} , which was greatly higher than the bimolecular dynamic quenching rate constant ($2 \times 10^{10} \text{ L mol}^{-1} \text{ s}^{-1}$) (Patar, Jalan et al. 2024), indicating a static quenching of the binding of rhamnazin to HSA.

3.1.2. Determination of the binding parameters

The binding parameters were calculated using modified Stern-Volmer Eq. (3) (Wang, Wang et al. 2023):

$$\log F_0 - F/F = \log K_b + n \log [C] \quad (3)$$

Table 1

Quenching, binding and thermodynamic parameters of HSA upon interaction with different concentrations of rhamnazin at 298/310/315 K.

T (K)	K_{sv} (10^5 L/mol)	k_q (10^{13} L/mol s $^{-1}$)	$\log K_b$ (L/mol)	n	ΔH° (kJ/mol)	ΔS° (J/mol K $^{-1}$)	ΔG° (kJ/mol)
298	2.12	2.12	7.64	1.53	147.922	641.258	-43.172
310	1.63	1.63	8.42	1.73	147.922	641.258	-50.867
315	0.65	0.65	9.12	1.97	147.922	641.258	-54.073

where K_b and n are defined as the binding constant and number of the binding site of protein, respectively, which can be calculated by plotting $\log(F_0 - F/F)$ against $\log[C]$ (Fig. 2b). Table 1 summaries the outcomes obtained at three different temperatures of 298/310/315 K for the interaction of rhamnazin and HSA. The n values of HSA were estimated to be in the range of 1.5 to 2, revealing the presence of more than one binding site on HSA for binding to rhamnazin (Zeinabad, Kachooei et al. 2016). Also, it was seen that the K_b values increased upon elevating temperature, revealing the formation of a stable rhamnazin-HSA complex at 315 K.

3.1.3. Determination of thermodynamic parameters

The ligand-macromolecule interaction occurs through four main driving forces, including hydrophobic, hydrogen bonding, van der Waals, and electrostatic forces (Siddiqui, Ameen et al. 2021). The thermodynamic parameters [enthalpy change (ΔH°), entropy change (ΔS°), and Gibbs free energy (ΔG°)] determine the type of binding interactions. The association between thermodynamic changes and binding interaction has been well documented. It has been manifested that when both ΔH° and ΔS° values are positive, hydrophobic forces are involved in the interaction of proteins with ligands, while van der Waals forces and hydrogen bonding mainly contribute to the interaction mechanism when both these values are negative. Electrostatic forces are mainly involved in the formation of ligand-protein complexes when ΔH° and ΔS° show different negative and positive values. The Van't Hoff Eq. (4) could be used for determining ΔH° and ΔS° values if temperature changes is minimum (Liu, Wang et al. 2022):

$$\ln K_b = -\Delta H^\circ / RT + \Delta S^\circ / R \quad (4)$$

where R is the gas constant.

The straight line upon plotting $\ln K_b$ versus $1/T$ can be used to determine ΔH° and ΔS° values (Fig. 2c). Then, the Gibbs-Helmholtz Eq.

(4) can be used to determine ΔG° values (Mariño-Ocampo, Rodríguez et al. 2023):

$$\Delta G^\circ = \Delta H^\circ - T\Delta S^\circ \quad (5)$$

As depicted in Fig. 2c and tabulated in Table 1, the negative ΔG° values display the spontaneous interaction of rhamnazin and HSA. Moreover, due to the positive values of ΔH° and ΔS° , it can be deduced that the main driving force in the interaction of rhamnazin and HSA is the hydrophobic forces. An endothermic reaction is associated with the positive value of ΔH° and the increasing K_b values with elevating temperature (Siddiqui, Ameen et al. 2021).

3.2. Circular dichroism study

Circular dichroism (CD) has been utilized as a sensitive spectroscopic technique to analyze the secondary structural change of protein in the presence of ligands (Tongkanarak, Loupiac et al. 2024). In order to explore the secondary structural alterations of HSA triggered by rhamnazin, a far-UV CD (200–260 nm) study was performed. In fact, upon interaction of rhamnazin, intermolecular forces involved in the stability of HSA structure may undergo some partial or substantial rearrangement, leading to conformational changes in the protein which is detected by monitoring the chirality changes (Tongkanarak, Loupiac et al. 2024). Fig. 3 depicts the far-UV CD signals of HSA without and with increasing concentrations of rhamnazin. It is evident that ellipticity changes of native HSA show two minima centered at 208 and 222 nm, representing the characteristic minima of typical α -helix structure (Tongkanarak, Loupiac et al. 2024).

Upon the addition of rhamnazin, a notable increase in the ellipticity changes at minima was detected without any significant shift, indicating an increase in the helical content and stability of HSA. In fact, it was deduced that the α -helix content of HSA was increased from 51.35 % to

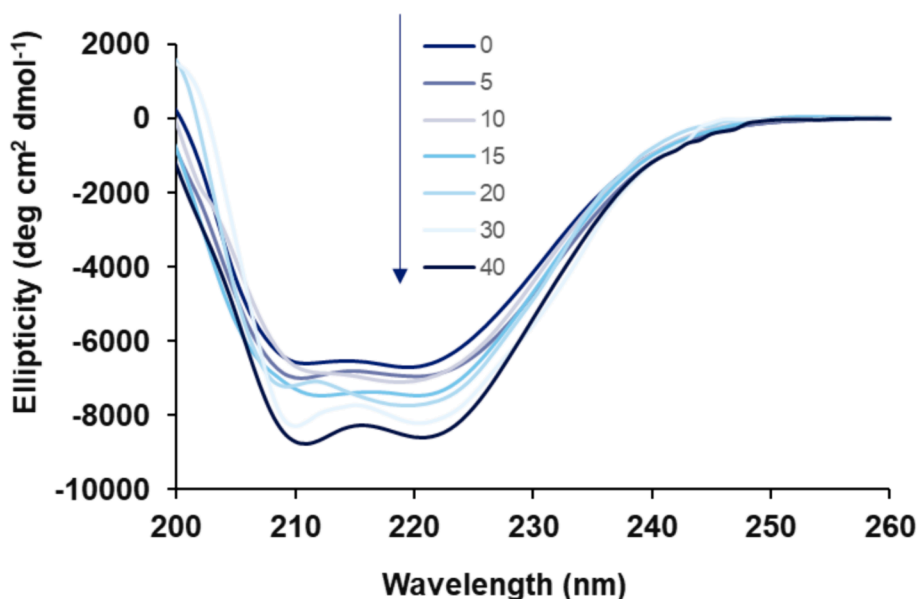


Fig. 3. Far-UV CD (200–260 nm) for the interaction of HSA (5 μ M) with different concentrations of rhamnazin ranging from 5 to 40 μ M at room temperature.

59.77 % upon increasing the concentration of rhamnazin from 0 to 40 μM , respectively, determined by CDNN software.

3.3. Molecular docking study

A theoretical simulation tool, molecular docking study, can be used to evaluate the nature of the ligand-receptor interaction (Fan, Wang et al. 2024). A molecular docking study was run to support experimental data about binding affinity and forces as well as amino acid residues at the binding pocket (Fig. 4a). Outcomes are detected from this assay, indicating that the rhamnazin shows a strong interaction and binding affinity ($\Delta G^\circ = -33.89 \text{ kJ/mol}$) with HSA at the domain B (Fig. 4b). The

rhamnazin conformer was revealed to interact with the active site residues R186, R145, R114, L112, E425, P110, L463, D108, V426, Y148, P147, H146, K190, S193, and F148 at domain B (Fig. 4c). Moreover, it was displayed that rhamnazin provided hydrophobic interaction with HSA through residue R145 (CB), whereas H146 is involved in the cation- π interaction, D108, R145 (NH1), and R197 are involved in the formation of hydrogen bonding. Data obtained from the molecular modeling study is in good agreement with the experimental outcomes, indicating the formation of rhamnazin-HSA binding mostly through hydrophobic forces.

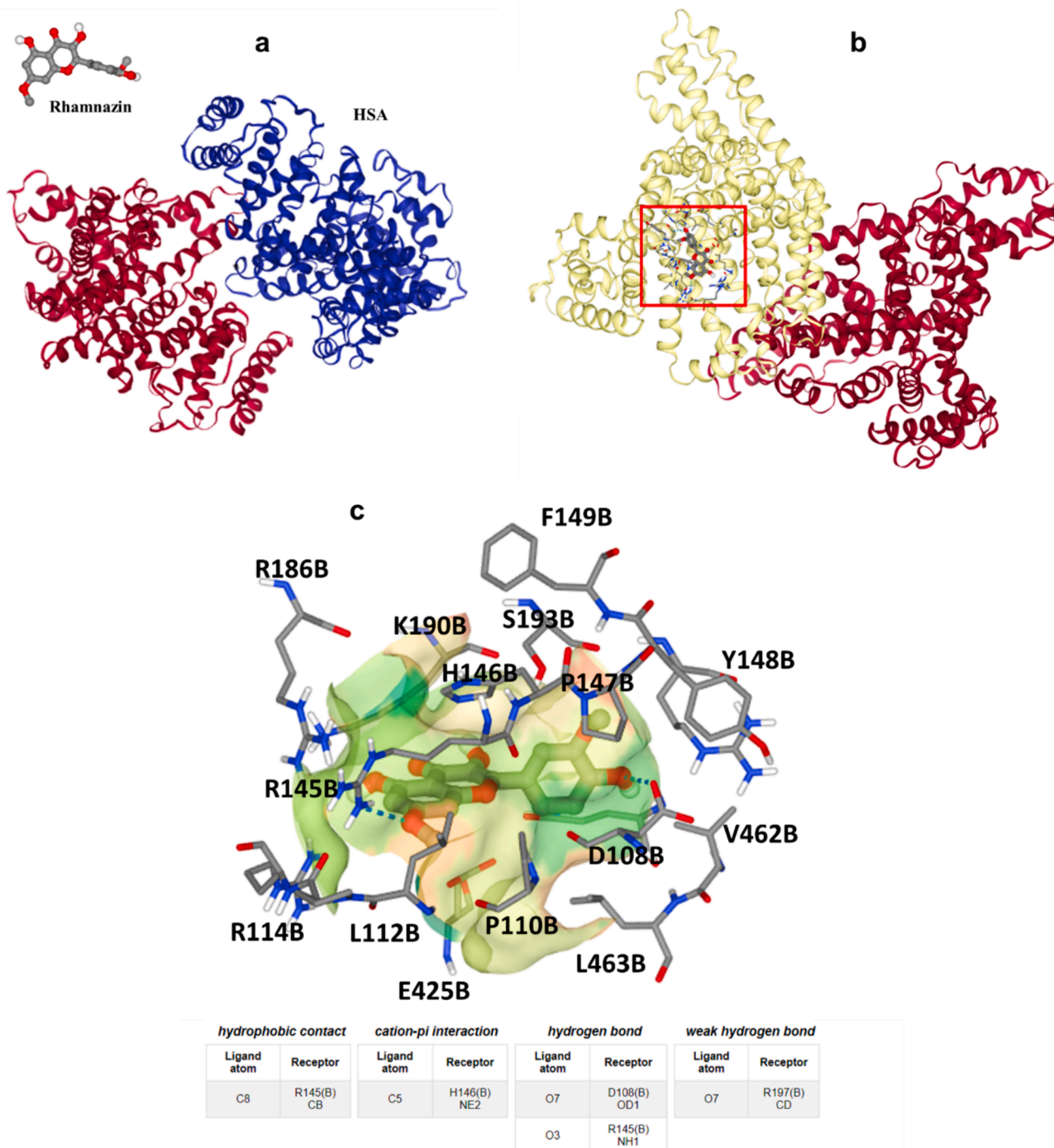


Fig. 4. (a) Rhamnazin and HSA structures, (b) binding site of HSA upon interaction with rhamnazin, (c) amino acid residues in the binding pocket.

3.4. Rhamnazin protects HK2 cells against H₂O₂-induced cytotoxicity

Fig. 5a displays the data obtained from the MTT assay, expressed as a percentage of cell viability in HK2 cells. For rhamnazin, it was shown that the maximum safe concentration at 10 μ M was achieved, while further increasing the rhamnazin concentration up to 50 μ M induced a significant reduction in cell viability (Fig. 5a). Therefore, rhamnazin with a concentration of 10 μ M was used for further studies. It was also shown that the HK2 cell viability was significantly ($***P < 0.001$) decreased after incubation of cells with 0.5 mM H₂O₂ for 24 h compared to control cell culture, as it was in good agreement with the previous study (Shahzad, Small et al. 2016). However, co-incubation of HK2 cells with rhamnazin with a concentration of 10 μ M for 24 h markedly ($^{\$}P < 0.01$) restored the cell viability compared with the H₂O₂-treated sample (Fig. 5b). Based on these data, it can be deduced that the rhamnazin (10 μ M) can protect cells against cytotoxicity induced by H₂O₂ (0.5 mM).

3.5. Rhamnazin protects HK2 cells against H₂O₂-induced oxidative stress

The potential of rhamnazin to inhibit the generation of ROS was assessed using the DCFH-DA assay. As illustrated in Fig. 6a the significant intracellular ROS generation in the cells exposed to H₂O₂ (0.5 mM) was potentially inhibited upon co-incubation of cells with H₂O₂ (0.5 mM) and rhamnazin (10 μ M) compared to the H₂O₂-treated group. Furthermore, the activities of the antioxidant enzymes, including CAT and SOD in HK2 cells were analyzed after 24 h of incubation with H₂O₂ (0.5 mM) and co-incubation with H₂O₂ (0.5 mM) and rhamnazin (10 μ M). As expected, H₂O₂ decreased SOD (Fig. 6b) and CAT (Fig. 6c) activities in HK2 cells and co-incubation of cells with H₂O₂ (0.5 mM) and rhamnazin (10 μ M) restored significantly the enzyme activities. Also, the analysis of GSH content (Fig. 6d) verified the antioxidant capacity of rhamnazin.

ROS production can be triggered by some mechanisms, including disruption of the mitochondrial membrane and activation of NADPH oxidase (Magnani and Mattevi 2019). ROS overproduction can result in some serious side effects against biomacromolecules, eventually triggering apoptosis (Juan, Pérez de la Lastra et al. 2021). As a result, any agent that reduces ROS production can be used as an antioxidant to counteract the cytotoxic effects of oxidative stress. In this study, we showed that rhamnazin can reduce ROS production by restoring the activity of antioxidant enzymes and biomolecules maintaining a redox state. It has been also shown that quercetin and rhamnazin can mitigate lipopolysaccharide-induced oxidative stress and inflammation in porcine intestinal cells (Karancsi, Kovács et al. 2022). Moreover, rhamnazin was shown to reduce traumatic brain injury through the inhibition of apoptosis and oxidative stress (Yang, Zhang et al. 2022).

3.6. Rhamnazin protects HK2 cells against H₂O₂-induced apoptosis

It was shown that incubation of HK2 cells with H₂O₂ (0.5 mM) induced apoptosis by upregulating caspase-3 and Bax mRNA and protein expression and downregulating Bcl-2 mRNA and protein expression (Fig. 7). However, rhamnazin (10 μ M) co-incubation decreased Bax mRNA expression (Fig. 7a) and increased Bcl-2 mRNA expression (Fig. 7b). Also, it was shown that rhamnazin (10 μ M) co-incubation mitigated the overexpression of caspase-3 mRNA induced by H₂O₂ (0.5 mM) in HK2 cells (Fig. 7c). Western blot analysis also verified that rhamnazin (10 μ M) co-incubation resulted in the downregulation of apoptotic proteins (Bax and cleaved caspase-3) and upregulation of anti-apoptotic protein (Bcl-2) (Fig. 7d).

In fact, this data revealed that rhamnazin can inhibit apoptosis through mitigation of ROS-associated Bax/Bcl-2 and caspase-3 signaling pathway stimulated by H₂O₂ in HK2 cells. Therefore, it may be discussed that rhamnazin can mitigate the induction of apoptosis in HK2 cells by regulating the mitochondrial pathway, decreasing Bax expression, and increasing Bcl-2 expression at both mRNA and protein levels as already shown by some other therapeutic compounds (Chang, Shen et al. 2014, Cao, Xu et al. 2021, Chen, Xie et al. 2023, Zhang, Tian et al. 2024). In accordance with our results, some other reports have shown that treatment with rhamnazin can control the induction of oxidative stress and apoptosis (Wu, Wang et al. 2022, Yang, Zhang et al. 2022, Ijaz, Mustafa et al. 2023).

3.7. Rhamnazin-induced cytotoxic effect in lung adenocarcinoma A549 cells

To assess the anti-lung cancer activity of rhamnazin, we assessed the MTT assay after interaction of lung adenocarcinoma A549 cells with different concentrations of rhamnazin for 24 h. The data suggested that rhamnazin induces cytotoxicity in lung adenocarcinoma A549 cells. Indeed, A549 cells were treated with different concentrations (1, 5, 10, 20, and 50 μ M) of rhamnazin, and the cell viability decreased from 100 % to 98.35 %, 71.74 %, 62.27 %, 52.18 %, and 34.32 %, respectively. Then the calculated IC₅₀ concentration was determined to be 10.03 μ M (Fig. 8a).

To detect whether the rhamnazin-induced cytotoxicity was mediated by apoptosis, the A549 cells were incubated with IC₅₀ concentrations of rhamnazin for 24 h, then the cells were subjected to flow cytometry.

As shown in Fig. 8b, the control cells (cells treated without rhamnazin) had 91.17 % lived cells with 6.21 % apoptotic cells. A549 cells treated with IC₅₀ concentration had a cell viability of 53.18 % upon treatment. The decrease in cell viability was accompanied by an elevation in the percentage of apoptotic cells to 27.15 % (Fig. 8b). Activation of the programmed cell death signaling pathway has been reported as an

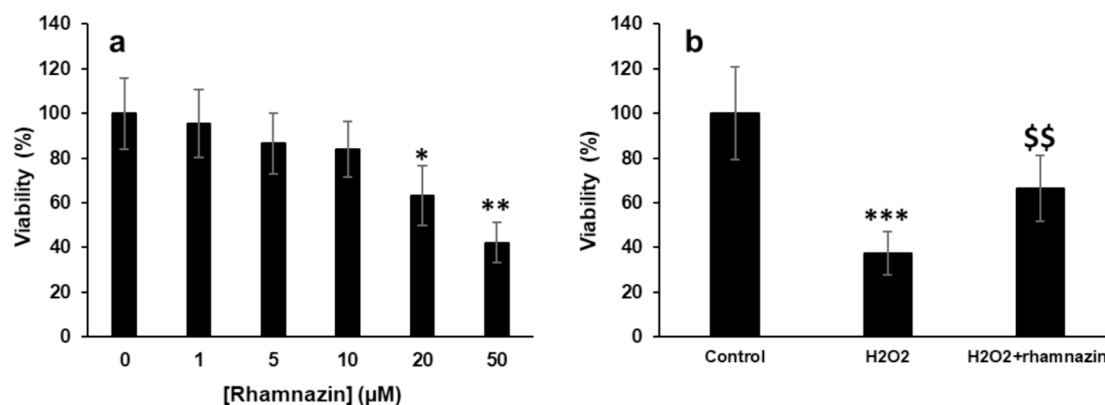


Fig. 5. Cell viability was assessed by the MTT assay. (a) Incubation of HK2 cells with increasing concentrations of rhamnazin for 24 h. (b) Incubation of cells with H₂O₂ (0.5 mM), or co-incubation of HK2 cells with H₂O₂ (0.5 mM) and rhamnazin (10 μ M) for 24 h. All data are expressed as means \pm SD. * $P < 0.05$, ** $P < 0.01$, *** $P < 0.001$, relative to untreated negative control cells; $^{\$}P < 0.01$ relative to H₂O₂-treated cells.

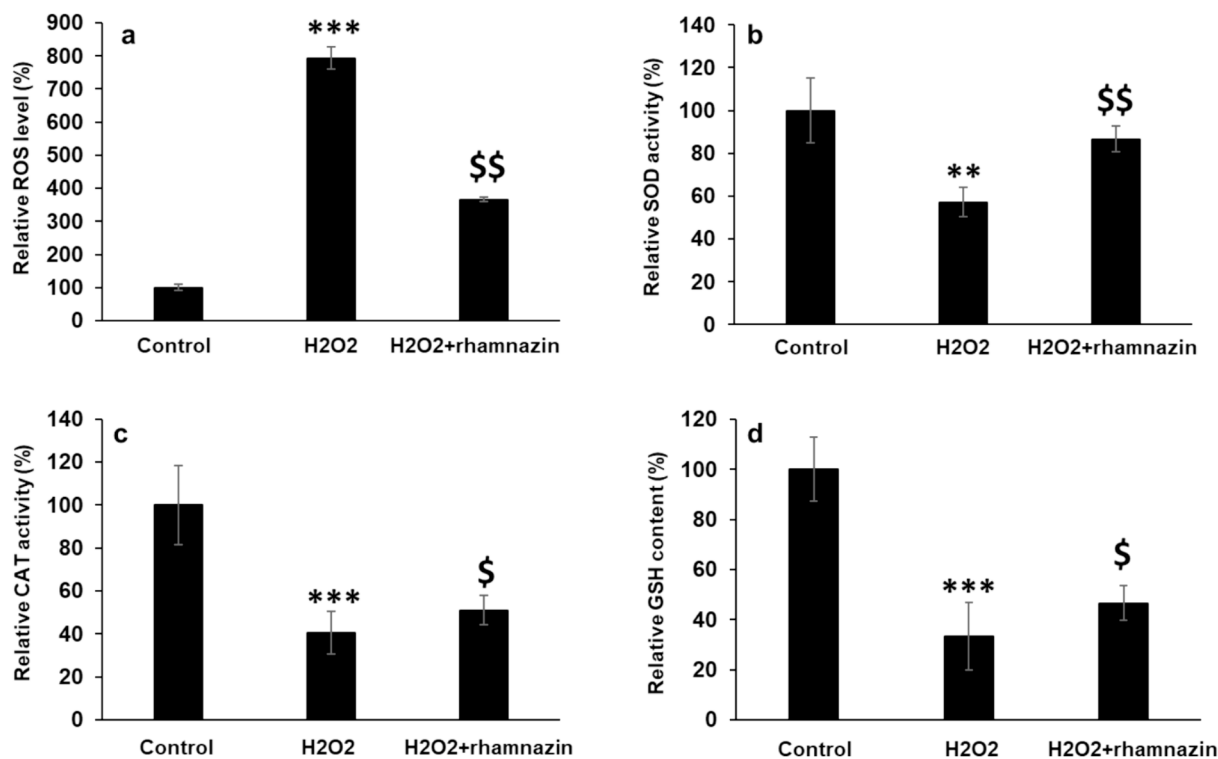


Fig. 6. Antioxidant properties of rhamnazin after incubation of HK2 cells with H₂O₂ (0.5 mM) or co-incubation with H₂O₂ (0.5 mM) and rhamnazin (10 μM) for 24 h. (a) ROS activity, (b) SOD activity, (c) CAT activity, (d) GSH content. All data are expressed as means ± SD. **P < 0.01, ***P < 0.001, relative to untreated negative control cells; \$P < 0.05, \$\$P < 0.01 relative to H₂O₂-treated cells.

important mechanism for reducing tumor formation and associated progression; thus, several anticancer agents have been recognized to potentially trigger apoptosis as a primer way of effect for their cytotoxic behavior (Carneiro and El-Deiry 2020, Biswas, Roy et al. 2024). Accordingly, in the present study, we found that the pathway of rhamnazin-induced anticancer effects is mediated by the induction of apoptosis.

3.8. Rhamnazin-induced signaling pathway in lung adenocarcinoma A549 cells

Following DNA damage, the tumor suppressor gene p53 could regulate the expression of several downstream proteins such as Bax, Bcl-2, and caspases (Amaral, Xavier et al. 2010, Wei, Wang et al. 2023). A high ratio of Bax/Bcl-2 can lead to the permeabilization of the outer mitochondrial membrane, causing the release of cytochrome *c* and the corresponding activation of caspase-9 and -3, to trigger the process of apoptosis (Kaloni, Diepstraten et al. 2023, Saddam, Paul et al. 2024, Singh, Anand et al. 2024). Hence, it is presumed that rhamnazin triggers DNA damage in A549 cells, resulting in the overexpression of p53 which then lead to regulation of the Bax, Bcl-2, and caspases.

A significant increase in the p53 mRNA expression was detected in the A549 cells treated with rhamnazin after 24 h of incubation (Fig. 9a). Bax (Fig. 9b) and Bcl-2 (Fig. 9c) mRNA expression in the treatment with rhamnazin after 24 h of incubation increased and reduced, respectively, in comparison with the control. Also, there was a significant change in the upregulation of apoptotic caspase-3 mRNA in the treatment with rhamnazin after 24 h of incubation (Fig. 9 d).

The same data was also detected in the p53, Bax, Bcl-2, and cleaved caspase-3 protein levels in the A549 cells treated with rhamnazin after 24 h of incubation (Fig. 9 e-h).

Therefore, the data demonstrated that the anticancer effect of rhamnazin on lung adenocarcinoma A549 cells is linked with its capability to trigger apoptosis in the cells. The apoptosis induction by

rhamnazin in lung adenocarcinoma A549 cells might be based on a p53-dependent manner, via upregulation of apoptotic Bax and caspase-3 and down-regulation of anti-apoptotic Bcl-2. However, the cytotoxicity of rhamnazin should be evaluated against several normal cell lines *in vitro* and *in vivo* to recognize the selectivity of this compound on cancerous cells. Therefore, we might suggest that rhamnazin could be a potential O-methylated flavonol for the treatment of lung cancer in the future.

4. Conclusion

In this paper, a characterization of the rhamnazin-HSA binding interaction was done by different spectroscopic and theoretical studies. Also, the protective effects of rhamnazin against H₂O₂-induced oxidative stress and apoptosis in HK2 cells were evaluated by different cellular and molecular assays. Furthermore, the anticancer effects of rhamnazin toward lung adenocarcinoma A549 cells were evaluated. It was shown that strong binding of rhamnazin to HSA was based on a static quenching, where more than one binding site was located on HSA for rhamnazin. Also, it was displayed that rhamnazin induced some structural changes in HSA conformation which resulted in an increase in the α-helix content of protein. Molecular docking analysis verified that binding interaction occurs through involvement of a hydrophobic residue, R145. Cellular and molecular assays demonstrated that rhamnazin can restore cell viability in HK2 cells treated with H₂O₂ (0.5 mM) for 24 h, through the reduction of oxidative stress and apoptosis. Moreover, rhamnazin showed potential cytotoxicity on lung adenocarcinoma A549 cells through a p53-dependent manner. This study may provide useful information about the valuable exploring of the pharmacokinetic characteristics along with antioxidant and anti-lung cancer activities of rhamnazin. In fact, this data may assist in revealing the molecular mechanisms behind the therapeutic effects of rhamnazin, thereby improving its pharmacological, biosafety and clinical potency, which needs further *in vivo* assay in future studies.

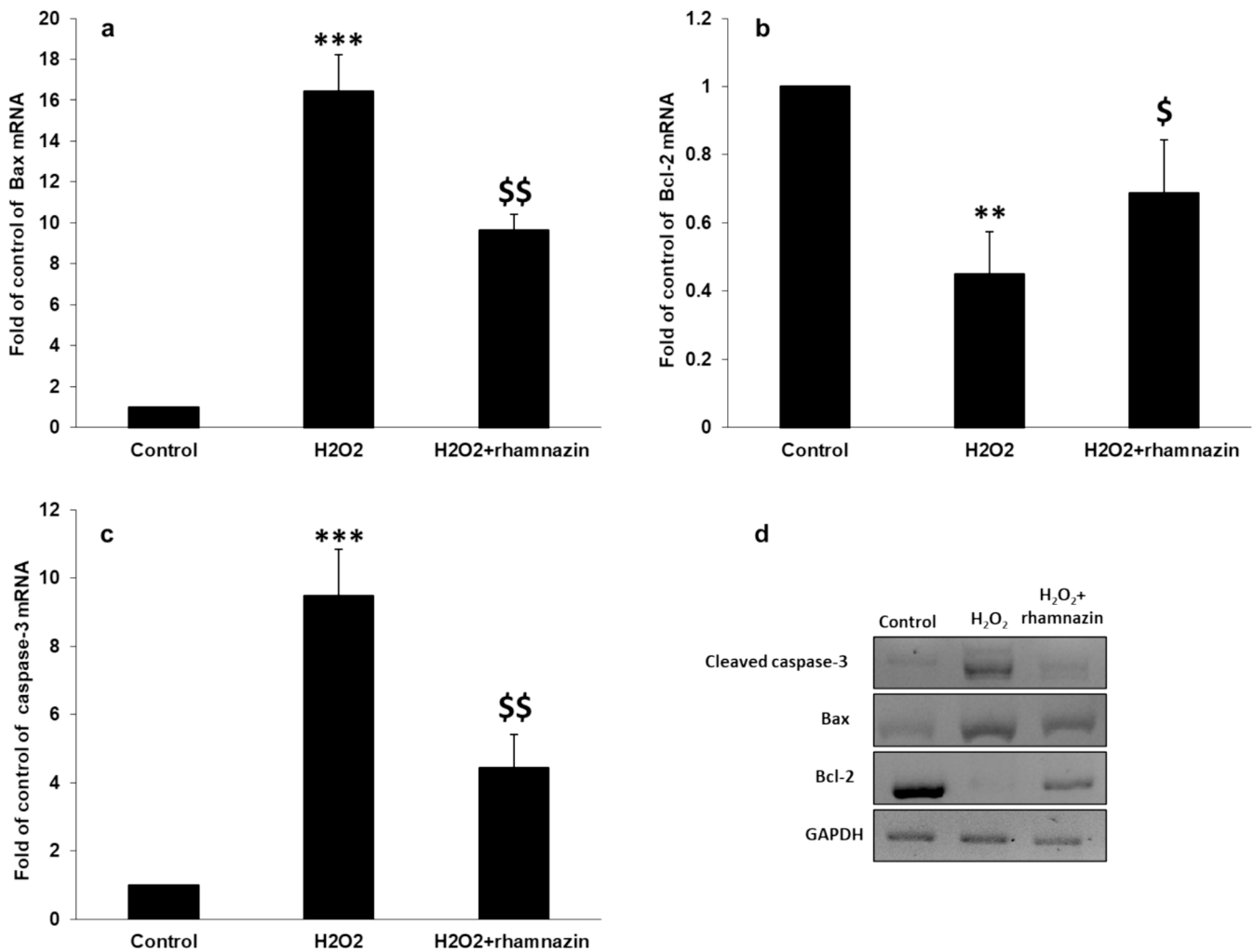


Fig. 7. Antiapoptotic properties of rhamnazin after incubation of HK2 cells with H₂O₂ (0.5 mM) or co-incubation with H₂O₂ (0.5 mM) and rhamnazin (10 μM) for 24 h. (a) Bax mRNA expression assay, (b) Bcl-2 mRNA expression assay, (c) caspase-3 mRNA expression assay, (d) western blot analysis. All data are expressed as means ± SD. **P < 0.01, ***P < 0.001, relative to untreated negative control cells; \$P < 0.05, \$\$P < 0.01 relative to H₂O₂-treated cells.

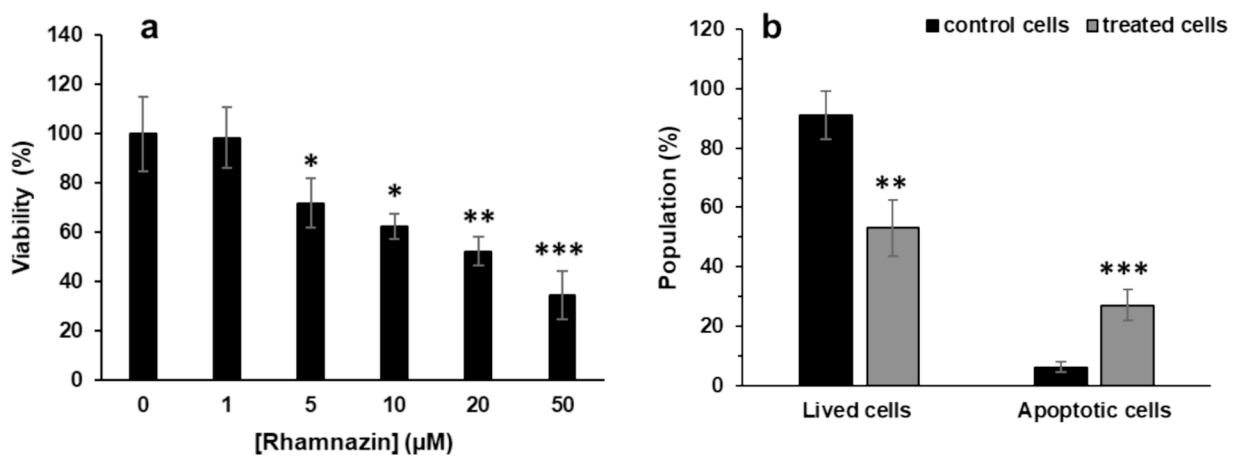


Fig. 8. (a) Cytotoxic effects of rhamnazin on lung adenocarcinoma A549 cells after incubation for 24 h, (b) flow cytometry analysis of lung adenocarcinoma A549 cells after interaction with IC₅₀ concentration of rhamnazin (10.00 μM) for 24 h. All data are expressed as means ± SD. *P < 0.05, **P < 0.01, ***P < 0.001, relative to untreated negative control cells.

CRedit authorship contribution statement

Zheng Chen: Writing – review & editing, Writing – original draft,

Methodology, Investigation, Formal analysis. **Yan Qiao:** Writing – review & editing, Validation, Supervision, Project administration, Investigation, Funding acquisition, Data curation, Conceptualization. **Yu**

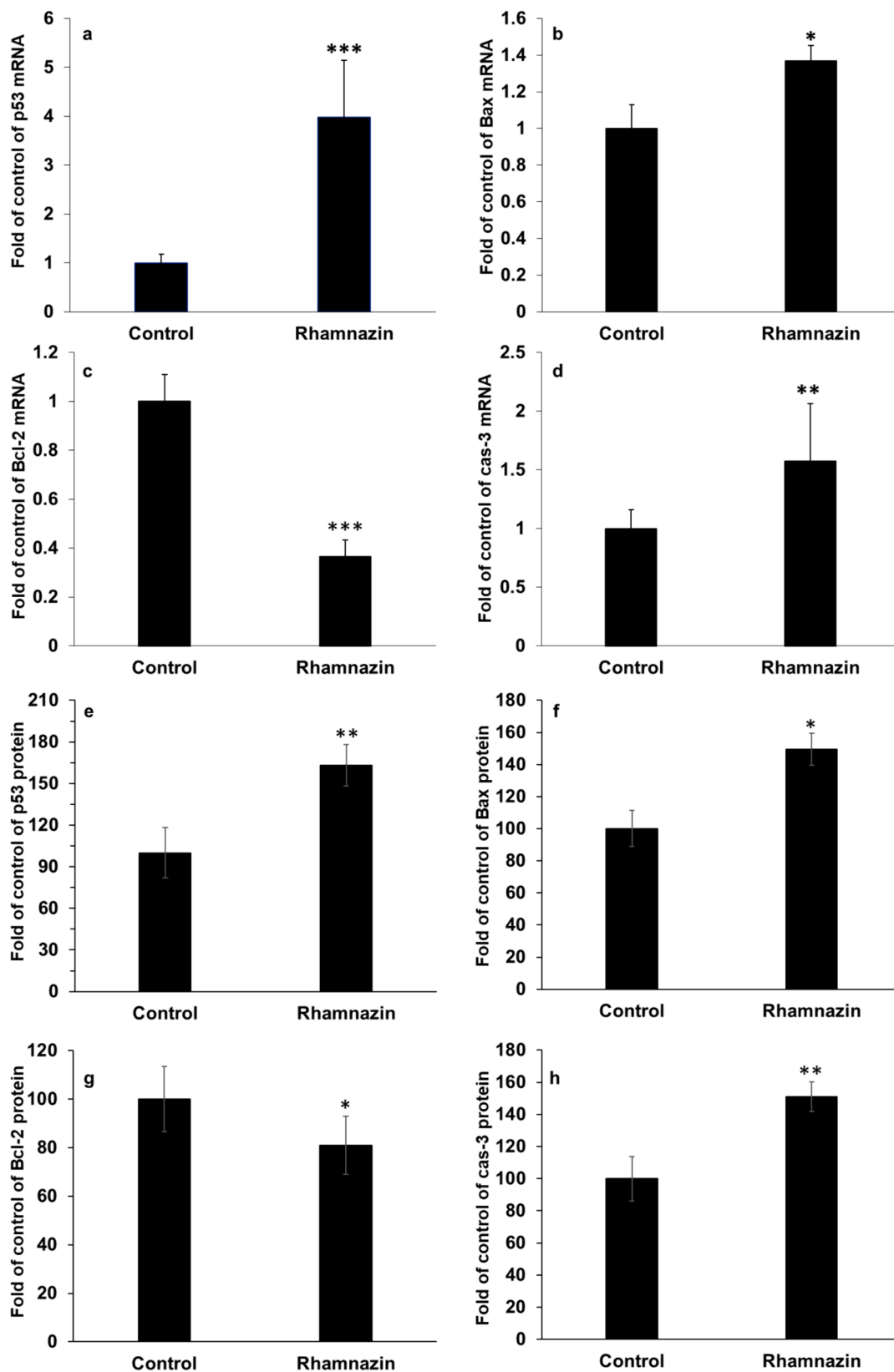


Fig. 9. Effect of IC₅₀ concentration of rhamnazin (10.00 μM) in lung adenocarcinoma A549 cells for 24 h on the (a) p53 mRNA expression, (b) Bax mRNA expression, (c) Bcl-2 mRNA expression, (d) caspase-3 (cas-3) mRNA expression, (e) p53 protein expression, (f) Bax protein expression, (g) Bcl-2 protein expression, (h) caspase-3 (cas-3) protein expression. All data are expressed as means ± SD. *P < 0.05, **P < 0.01, ***P < 0.001, relative to untreated negative control cells.

Chen: Writing – review & editing, Validation, Supervision, Project administration, Investigation, Funding acquisition, Data curation, Conceptualization. **Tingting Ma:** Writing – review & editing, Validation, Supervision, Project administration, Investigation, Funding acquisition, Data curation, Conceptualization. **Wei Li:** Writing – review & editing, Validation, Supervision, Project administration, Investigation, Funding acquisition, Data curation, Conceptualization. **Jianhong Xia:** Writing – review & editing, Validation, Supervision, Project administration, Investigation, Funding acquisition, Data curation, Conceptualization. **Yan Yan:** Writing – review & editing, Validation, Supervision, Project administration, Investigation, Funding acquisition, Data curation, Conceptualization. **Qian Jiang:** Writing – review & editing, Validation, Supervision, Project administration, Investigation, Funding acquisition, Data curation, Conceptualization. **Liqing Zhou:** Writing – review & editing, Validation, Supervision, Project administration, Investigation, Funding acquisition, Data curation, Conceptualization.

Declaration of competing interest

The authors declare that they have no known competing financial interests or personal relationships that could have appeared to influence the work reported in this paper.

Acknowledgments

This work was supported by no external funding.

References

- Aguilar, T.A.F., Navarro, B.C.H., Pérez, J.A.M., 2016. "Endogenous antioxidants: a review of their role in oxidative stress." *A master regulator of oxidative stress-the transcription factor nrf2*: 3-20.
- Akram, S.M., Al-Saffar, A.Z., Hadi, N.A., Akram, S.M., 2022. Utilization of novel lectin-conjugated Au nanoparticles as Thomsen-Friedenreich onco-antigen target for in vitro cytotoxicity and apoptosis induction in leukemic cell line. *Life Sci.* 311, 121163.
- Alam, P., Chaturvedi, S.K., Anwar, T., Siddiqi, M.K., Ajmal, M.R., Badr, G., Mahmoud, M. H., Khan, R.H., 2015. Biophysical and molecular docking insight into the interaction of cytosine β -D arabinofuranoside with human serum albumin. *J. Lumin.* 164, 123–130.
- Ali, M.S., Al-Lohedan, H.A., 2018. Spectroscopic and computational evaluation on the binding of safranal with human serum albumin: role of inner filter effect in fluorescence spectral correction. *Spectrochim. Acta A Mol. Biomol. Spectrosc.* 203, 434–442.
- Amaral, J.D., Xavier, J.M., Steer, C.J., Rodrigues, C.M., 2010. The role of p53 in apoptosis. *Discov. Med.* 9 (45), 145–152.
- Biswas, U., Roy, R., Ghosh, S., Chakrabarti, G., 2024. The interplay between autophagy and apoptosis: its implication in lung cancer and therapeutics. *Cancer Lett.* 216662.
- Cao, Y., Xu, J., Cui, D., Liu, L., Zhang, S., Shen, B., Wu, Y., Zhang, Q., 2021. Protective effect of carnosine on hydrogen peroxide-induced oxidative stress in human kidney tubular epithelial cells. *Biochem. Biophys. Res. Commun.* 534, 576–582.
- Carneiro, B.A., El-Deiry, W.S., 2020. Targeting apoptosis in cancer therapy. *Nat. Rev. Clin. Oncol.* 17 (7), 395–417.
- Chang, C.-Y., Shen, C.-Y., Kang, C.-K., Sher, Y.-P., Sheu, W.-H.-H., Chang, C.-C., Lee, T.-H., 2014. Taurine protects HK-2 cells from oxidized LDL-induced cytotoxicity via the ROS-mediated mitochondrial and p53-related apoptotic pathways. *Toxicol. Appl. Pharmacol.* 279 (3), 351–363.
- Chen, Q., Liu, Z., 2016. Albumin carriers for cancer theranostics: a conventional platform with new promise. *Adv. Mater.* 28 (47), 10557–10566.
- Chen, P., Liu, Y., Wen, Y., Zhou, C., 2022. Non-small cell lung cancer in China. *Cancer Commun.* 42 (10), 937–970.
- Chen, J., Xie, C., Yu, Z., 2023. Protective effect of dihydromyricetin against lipopolysaccharide-induced HK2 cells by upregulating HIF-1 α . *Biotechnol. Genet. Eng. Rev.* 1–11.
- dos Santos Rodrigues, F.H., Delgado, G.G., da Costa, T.S., Tasic, L., 2023. Applications of fluorescence spectroscopy in protein conformational changes and intermolecular contacts. *BBA Advances* 3, 100091.
- Fan, S.-H., Wang, W.-Q., Zhou, Y.-W., Gao, X.-J., Zhang, Q., Zhang, M.-H., 2024. Research on the Interaction Mechanism and Structural Changes in Human Serum Albumin with Hispidin Using Spectroscopy and Molecular Docking. *Molecules* 29 (3), 655.
- Fossum, C.J., Johnson, B.O.V., Golde, S.T., Kielman, A.J., Finke, B., Smith, M.A., Lowater, H.R., Laatsch, B.F., Bhattacharyya, S., Hati, S., 2023. Insights into the mechanism of tryptophan fluorescence quenching due to synthetic crowding agents: A combined experimental and computational study. *ACS Omega* 8 (47), 44820–44830.
- Ghosh, T., Bhadra, K., 2024. A mini review on human serum albumin-natural alkaloids interaction and its role as drug carrier. *J. Biomol. Struct. Dyn.* 1–18.
- Ijaz, M.U., Mustafa, S., Ain, Q.U., Hamza, A., Ali, S., 2023. "Rhamnazin ameliorates 2, 3, 7, 8-tetrachlorodibenzo-p-dioxin-evoked testicular toxicity by restoring biochemical, spermatogenic and histological profile in male albino rats. *Human & Experimental Toxicology* 42: 09603271231205859.
- Iqbal, M.J., Kabeer, A., Abbas, Z., Siddiqui, H.A., Calina, D., Sharifi-Rad, J., Cho, W.C., 2024. Interplay of oxidative stress, cellular communication and signaling pathways in cancer. *Cell Commun. Signal.* 22 (1), 7.
- Jomova, K., Raptova, R., Alomar, S.Y., Alwaseel, S.H., Nepovimova, E., Kuca, K., Valko, M., 2023. Reactive oxygen species, toxicity, oxidative stress, and antioxidants: chronic diseases and aging. *Arch. Toxicol.* 97 (10), 2499–2574.
- Juan, C.A., Pérez de la Lastra, J.M., Plou, F.J., Pérez-Lebeña, E., 2021. The chemistry of reactive oxygen species (ROS) revisited: outlining their role in biological macromolecules (DNA, lipids and proteins) and induced pathologies. *Int. J. Mol. Sci.* 22 (9), 4642.
- Kaloni, D., Diepstraten, S.T., Strasser, A., Kelly, G.L., 2023. BCL-2 protein family: Attractive targets for cancer therapy. *Apoptosis* 28 (1), 20–38.
- Karancsi, Z., Kovács, D., Palkovicsné Pézsa, N., Gálfi, P., Jerzsele, Á., Farkas, O., 2022. The impact of quercetin and its methylated derivatives 3-o-methylquercetin and rhamnazin in lipopolysaccharide-induced inflammation in porcine intestinal cells. *Antioxidants* 11 (7), 1265.
- Kenoth, R. and R. K. Kamlekar (2022). Steady-state fluorescence spectroscopy as a tool to monitor protein/ligand interactions. *Optical Spectroscopic and Microscopic Techniques: Analysis of Biological Molecules*, Springer: 35-54.
- Kim, Y.J., 2016. Rhamnazin inhibits LPS-induced inflammation and ROS/RNS in raw macrophages. *J. Nutr. Health* 49 (5), 288–294.
- Kishi, S., Nagasu, H., Kidokoro, K., Kashiwara, N., 2024. Oxidative stress and the role of redox signalling in chronic kidney disease. *Nat. Rev. Nephrol.* 20 (2), 101–119.
- Kong, F., Zhang, R., Zhao, X., Zheng, G., Wang, Z., Wang, P., 2017. Resveratrol raises in vitro anticancer effects of paclitaxel in NSCLC cell line A549 through COX-2 expression. *Korean J. Physiol. Pharmacol.: Off. J. Korean Physiol. Soc. Korean Soc. Pharmacol.* 21 (5), 465.
- Kratz, F., 2014. A clinical update of using albumin as a drug vehicle—a commentary. *J. Control. Release* 190, 331–336.
- Leilabadi-Asl, A., Divsalar, A., Karizak, A.Z., Fateminasab, F., Shityakov, S., Moghadam, M.E., Saboury, A.A., 2024. Unraveling the binding interactions between two Pt (II) complexes of aliphatic glycine derivatives with human serum albumin: a comprehensive computational and multi-spectral investigation. *Int. J. Biol. Macromol.* 266, 131298.
- Liu, H., Wang, J., He, Y., Zhang, W., Lei, L., Chen, L., Chen, Y., Zhu, J., Tu, J., Li, K., 2022. Investigation of the binding properties of 3, 4-dihydroxybenzaldehyde from *Salvia miltiorrhiza* (Bunge) with human serum albumin via multi-spectroscopic and molecular docking techniques. *BioResources* 17 (2), 2680.
- Magnani, F., Mattevi, A., 2019. Structure and mechanisms of ROS generation by NADPH oxidases. *Curr. Opin. Struct. Biol.* 59, 91–97.
- Marino-Ocampo, N., Rodríguez, D.F., Guerra Díaz, D., Zúñiga-Núñez, D., Duarte, Y., Fuentealba, D., Zacconi, F.C., 2023. Direct oral FXa inhibitors binding to human serum albumin: spectroscopic, calorimetric, and computational studies. *Int. J. Mol. Sci.* 24 (5), 4900.
- Mei, F., Liu, Y., Zheng, S., 2022. Rhamnazin inhibits hepatocellular carcinoma cell aggressiveness in vitro via glutathione peroxidase 4-dependent ferroptosis. *Tohoku J. Exp. Med.* 258 (2), 111–120.
- Patar, M., Jalan, A., Moyon, N.S., 2024. A spectroscopic and molecular docking study on the interaction of 2'-hydroxyflavanone with bovine serum albumin. *Phys. Chem. Res.* 12 (3), 709–727.
- Patel, K., Kumar, V., Rahman, M., Verma, A., Patel, D.K., 2018. Rhamnazin: A systematic review on ethnopharmacology, pharmacology and analytical aspects of an important phytochemistry. *Curr. Tradit. Med.* 4 (2), 120–127.
- Quinlan, G.J., Martin, G.S., Evans, T.W., 2005. Albumin: biochemical properties and therapeutic potential. *Hepatology* 41 (6), 1211–1219.
- Roy, S., Tapan Kumar Das, K., Ponra, S., Ghosh, T., 2016. Interaction of bovine serum albumin with synthetic spiropyrimidines. *Adv. Mater. Lett.* 7(1), 65–70.
- Saddam, M., Paul, S.K., Habib, M.A., Fahim, M.A., Mimi, A., Islam, S., Paul, B., Helal, M. M.U., 2024. Emerging biomarkers and potential therapeutics of the BCL-2 protein family: the apoptotic and anti-apoptotic context. *Egypt. J. Med. Human Genet.* 25 (1), 12.
- Shahzad, M., Small, D.M., Morais, C., Wojcikowski, K., Shabbir, A., Gobe, G.C., 2016. Protection against oxidative stress-induced apoptosis in kidney epithelium by *Angelica* and *Astragalus*. *J. Ethnopharmacol.* 179, 412–419.
- Siddiqui, S., Ameen, F., ur Rehman, S., Sarwar, T., Tabish, M., 2021. Studying the interaction of drug/ligand with serum albumin. *J. Mol. Liquids* 336, 116200.
- Singh, N., Anand, P., Bhumika, K., 2024. Targeting apoptotic cell death in cancer therapy: chemotherapeutic approaches. *Int. J. Pharm. Drug Des.* 77–87.
- Small, D.M., Morais, C., Coombes, J.S., Bennett, N.C., Johnson, D.W., Gobe, G.C., 2014. Oxidative stress-induced alterations in PPAR- γ and associated mitochondrial destabilization contribute to kidney cell apoptosis. *Am. J. Physiol.-Renal Physiol.* 307 (7), F814–F822.
- Tayyab, S., Feroz, S.R., 2021. Serum albumin: Clinical significance of drug binding and development as drug delivery vehicle. *Adv. Protein Chem. Struct. Biol.* 123, 193–218.
- Tongkanarak, K., C. Loupiac, F. Neiers, O. Chamblin, Srichana, T., 2024. Evaluating the biomolecular interaction between delamanid/formulations and human serum albumin by fluorescence, CD spectroscopy and SPR: effects on protein conformation, kinetic and thermodynamic parameters. *Colloids Surf. B: Biointerfaces*: 113964.

- Van de Weert, M., Stella, L., 2011. Fluorescence quenching and ligand binding: a critical discussion of a popular methodology. *J. Mol. Struct.* 998 (1–3), 144–150.
- Wang, M., Wang, Y.-C., Bai, Z.-L., Sui, Y., Yin, D., Yin, H., 2023. Exploring thyroxine binding globulin structural changes and its release from human hepatoblastoma cells upon interaction with silica particles: a prelude to unrevealing the mechanism of thyroid hormone dysregulation. *Int. J. Biol. Macromol.* 251, 126240.
- Wei, H., Wang, H., Wang, G., Qu, L., Jiang, L., Dai, S., Chen, X., Zhang, Y., Chen, Z., Li, Y., 2023. Structures of p53/BCL-2 complex suggest a mechanism for p53 to antagonize BCL-2 activity. *Nat. Commun.* 14 (1), 4300.
- Wu, G., Dai, X., Li, X., Jiang, H., 2017. Antioxidant and anti-inflammatory effects of rhamnazin on lipopolysaccharide-induced acute lung injury and inflammation in rats. *Afr. J. Tradit. Complement. Altern. Med.* 14 (4), 201–212.
- Wu, X.Y., Wang, T., Hu, H.X., Zhang, K., Zhao, Y., Zhao, B.B., Lou, H.X., Wang, X.N., Shen, T., 2022. The alleviative effect of flavonol-type Nrf2 activator rhamnazin from *Physalis alkekengi* L. var. *franchetii* (Mast.) Makino on pulmonary disorders. *Phytother. Res.* 36 (4), 1692–1707.
- Yamasaki, K., Chuang, V.T.G., Maruyama, T., Otagiri, M., 2013. Albumin–drug interaction and its clinical implication. *Biochimica et Biophysica Acta (BBA)-General Subjects* 1830 (12), 5435–5443.
- Yang, B., Zhang, R., Sa, Q., Du, Y., 2022. Rhamnazin ameliorates traumatic brain injury in mice via reduction in apoptosis, oxidative stress, and inflammation. *Neuroimmunomodulation* 29 (1), 28–35.
- Yu, Y., Cai, W., Pei, C.-G., Shao, Y., 2015. Rhamnazin, a novel inhibitor of VEGFR2 signaling with potent antiangiogenic activity and antitumor efficacy. *Biochem. Biophys. Res. Commun.* 458 (4), 913–919.
- Yuan, T., N. Yang, W. Bi, J. Zhang, X. Li, L. Shi, Y. Liu and X. Gao, 2021. Protective role of sulodexide on renal injury induced by limb ischemia-reperfusion. *Evidence-Based Complement. Alternat. Med.* 2021.
- Yuan, Q., Tang, B., Zhang, C., 2022. Signaling pathways of chronic kidney diseases, implications for therapeutics. *Signal Transduct. Target. Ther.* 7 (1), 182.
- Zeinabad, H.A., Kachooei, E., Saboury, A.A., Kostova, I., Attar, F., Vaezzadeh, M., Falahati, M., 2016. Thermodynamic and conformational changes of protein toward interaction with nanoparticles: a spectroscopic overview. *RSC Adv.* 6 (107), 105903–105919.
- Zhang, Q., Tian, L., Hu, Y., Jiang, W., Wang, X., Chen, L., Cheng, S., Ying, J., Jiang, B., Zhang, L., 2024. Aristolochic acid I aggravates oxidative stress-mediated apoptosis by inhibiting APE1/Nrf2/HO-1 signaling. *Toxicol. Mech. Methods* 34 (1), 20–31.